

Inversion of Remote Sensing Reflectance to Obtain Phytoplankton Community Size Structure

Colleen B. Mouw¹ & James A. Yoder²

¹Graduate School of Oceanography, University of Rhode Island, cmouw@gso.uri.edu
²Woods Hole Oceanographic Institution

I. Introduction

Size distribution is a major biological factor that governs the functioning of pelagic food webs. Despite the physiological and taxonomic variability in a phytoplankton assemblage, Ciotti et al. (2002) described a strong co-variation of the size of the dominant organism and several factors controlling the spectral shape of the absorption coefficient of phytoplankton (eqn. 1). In this way, the phytoplankton size parameter (S_f ; percentage of picoplankton) can be retrieved from remotely sensed reflectance (R_{rs} , sr⁻¹) through its relation to absorption (a^*_{ph}).

$$a^*_{ph}(\lambda) = [S_f \times a^*_{pico}(\lambda)] + [(1-S_f) a^*_{micro}(\lambda)] \quad (1)$$

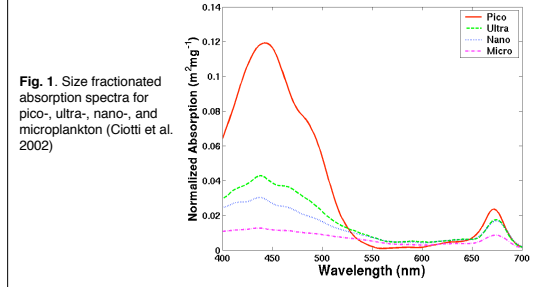


Fig. 1. Size fractionated absorption spectra for pico-, ultra-, nano-, and microplankton (Ciotti et al. 2002)

II. Theory of Inversion

The inversion relates reflectance spectra ($R_{rs}(\lambda)$) to the inherent optical properties (IOPs) of the water, in particular total absorption (a) and backscattering (b_b) coefficients. The inversion of $R_{rs}(\lambda)$ to obtain S_f is done by fitting the modeled IOPs to $R_{rs}(\lambda)$ by non-linear least-squares optimization according to a modified Garver-Siegel-Maritorena 2001 inversion model (Maritorena et al. 2002).

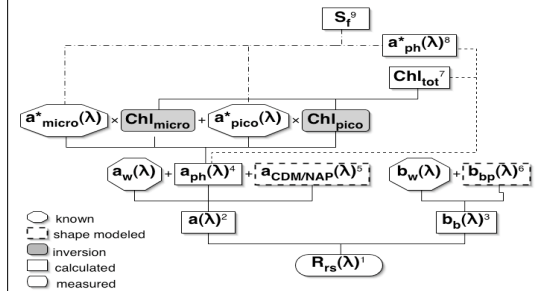


Fig. 2. Flow schematic of the inversion calculation to estimate the phytoplankton size parameter (S_f). The previously published equations integrated into the calculation are (1) $R_{rs}(\lambda) = b_b(\lambda)/(a(\lambda) + b_b(\lambda))$; (2) $a(\lambda) = a_w(\lambda) + a_{ph}(\lambda) + a_{CDMNAP}(\lambda)$; (3) $b_b(\lambda) = b_{wp}(\lambda) + b_{bp}(\lambda)$; (4) $a_{ph}(\lambda) = [a^*_{pico}(\lambda)(Chl_{pico})] + [a^*_{micro}(\lambda)(Chl_{pico})]$; (5) $a_{CDMNAP}(\lambda) = a_{CDMNAP}(\lambda_0) \exp[-S(\lambda - \lambda_0)]$; (6) $b_{bp}(\lambda) = b_{bp}(\lambda_0)(\lambda/\lambda_0)^{-\eta}$; (7) $Chl_{tot} = Chl_{pico} + Chl_{micro}$; (8) $a^*_{ph}(\lambda) = a^*_{ph}(\lambda)Chl_{tot}$; (9) $S_f = [a^*_{ph}(\lambda) - a^*_{micro}(\lambda)]/[a^*_{pico}(\lambda) + a^*_{micro}(\lambda)]$. The shape factors η and S are assumed known and constant (Maritorena et al. 2002).

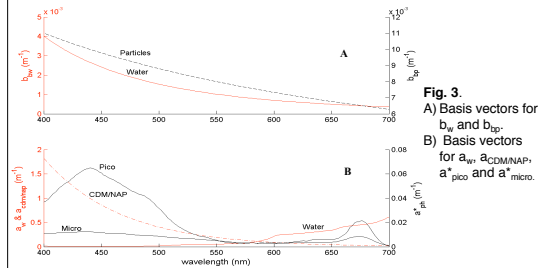


Fig. 3. A) Basis vectors for b_w and b_{bp} . B) Basis vectors for a^*_w , a^*_{CDMNAP} , a^*_{pico} and a^*_{micro} .

III. Feasibility - Forward Modeling

Sensitivity of $R_{rs}(\lambda)$ to changes in S_f were examined using Hydrolight 4.2 to calculate $R_{rs}(\lambda)$ (Fig. 4) from a three-component model consisting of absorption and scattering properties of water, phytoplankton, and CDM/NAP (Fig. 3). The Ciotti et al. (2002) a^*_{pico} and a^*_{micro} vectors were used to define phytoplankton absorption.

Radiometer Sensitivity and Detection

The difference between pico- and microplankton $R_{rs}(\lambda)$ ($\Delta R_{rs}(\lambda)$) were calculated and reduced to 10% of the original signal to account for atmospheric loss (degraded mean $\Delta R_{rs} = 2.51 \times 10^{-4}$ sr⁻¹). The least sensitive channel of SeaWiFS (412 nm, $NEAR_{rs} = 5.4 \times 10^{-5}$ sr⁻¹) is an order of magnitude more sensitive than $\Delta R_{rs}(\lambda)$ indicating the inversion methodology to obtain S_f can be successful with current satellite instrument specifications.

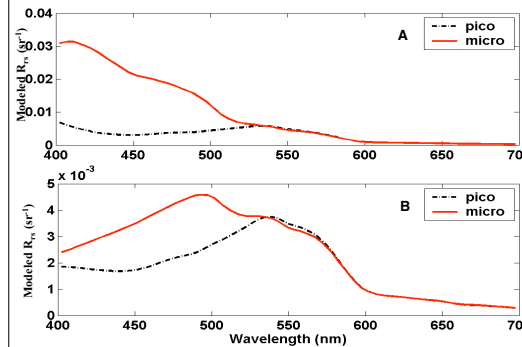


Fig. 4. Example of Hydrolight forward model simulations for pico- and microplankton size classes. A) Chl = 1 µg/L, $a_{CDMNAP} = 0$ m⁻¹. B) Chl = 1 µg/L, $a_{CDMNAP} = 0.1$ m⁻¹.

IV. Preliminary Validation

Relative biomass proportions of pico-, nano-, and microplankton can be estimated from the concentrations of taxonomically significant pigments (Bricaud et al. 2004). HPLC pigments collected from the Atlantic Meridional Transect (AMT) (Werdell and Bailey 2002; Werdell et al. 2003) are used to characterize *in situ* percentage of picoplankton across diverse ecological regions. Phytoplankton size estimated from AMT pigments are compared to S_f satellite inversion retrievals.

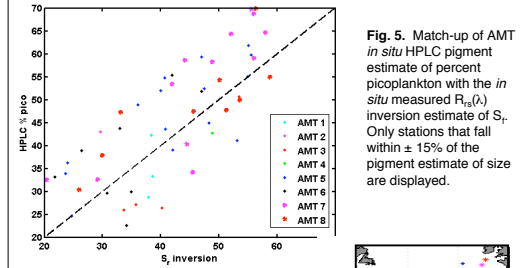


Fig. 5. Match-up of AMT *in situ* HPLC pigment estimate of percent picoplankton with the *in situ* measured $R_{rs}(\lambda)$ inversion estimate of S_f . Only stations that fall within $\pm 15\%$ of the pigment estimate of size are displayed.

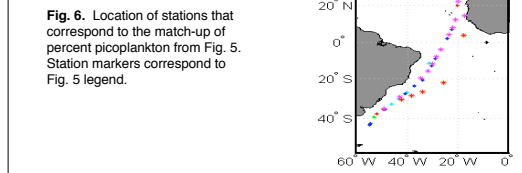


Fig. 6. Location of stations that correspond to the match-up of percent picoplankton from Fig. 5. Station markers correspond to Fig. 5 legend.

V. Application to Satellite Imagery

SeaWiFS high-resolution level 1a $R_{rs}(\lambda)$ imagery corresponding to the date and location of the AMT *in situ* stations were processed to level 2 and inverted to obtain an estimate of S_f .

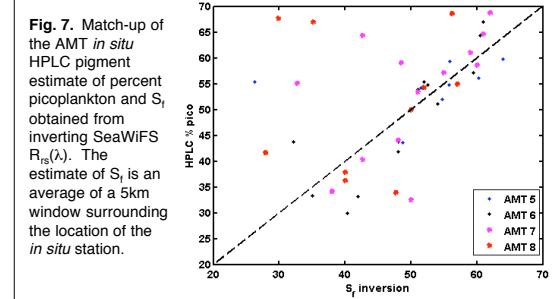


Fig. 7. Match-up of the AMT *in situ* HPLC pigment estimate of percent picoplankton and S_f obtained from inverting SeaWiFS $R_{rs}(\lambda)$. The estimate of S_f is an average of a 5km window surrounding the location of the *in situ* station.

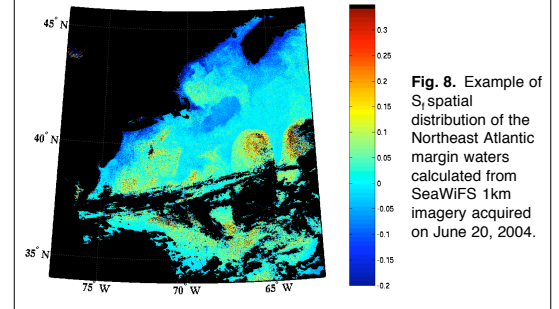


Fig. 8. Example of S_f spatial distribution of the Northeast Atlantic margin waters calculated from SeaWiFS 1km imagery acquired on June 20, 2004.

VI. Conclusions

Initial results are promising but significant improvement is still needed. The inversion scheme is yielding noisy estimates of S_f in comparison to the *in situ* AMT HPLC pigment estimate of picoplankton. The imagery inversion estimate of S_f displays better retrieval at higher percentage of picoplankton in a given community. The spatial patterns in the imagery are reasonable, however, the estimate of the size parameter still needs improvement. Further tuning of the a_{CDMNAP} (S) and b_{bp} (η) shape coefficients and the overall inversion approach may be required. The methodology has implications for new production models and carbon cycling investigations.

References

Ciotti, A., M. Lewis, and J. Callen. 2002. Assessment of the relationship between dominant cell size in natural phytoplankton communities and the spectral shape of the absorption coefficient. *Limnol. Oceanogr.* 47: 404-417.
 Bricaud, A., H. Claustre, J. Ras, and K. Oubelkheir. 2004. Natural variability of phytoplanktonic absorption in oceanic waters: Influence of size structure of algal populations. *J. Geophys. Res.* 109: doi:10.1029/2004JC002419.
 Maritorena, S., D. Siegel, and A. Peterson. 2002. Optimization of a semi-analytical ocean color model for global-scale applications. *Applied Optics.* 41: 2705-2714.
 Werdell, P.J., S.W. Bailey, G.S. Fargion, C. Pietras, K.D. Knobelspiess, G.C. Feldman, and C.R. McClain. 2003. Unique data repository facilitates ocean color satellite validation. *EOS Trans. AGU.* 84, 38, 377.
 Werdell, P.J., and S.W. Bailey. 2002. The SeaWiFS Bio-optical Archive and Storage System (SeaBASS): Current architecture and implementation. *NASA Tech. Memo. 2002-21617*, G.S. Fargion and C.R. McClain, Eds., NASA Goddard Space Flight Center, Greenbelt, Maryland, 45 pp.

Acknowledgements

The AMT data was acquired through the SeaWiFS Bio-optical Archive and Storage System (SeaBASS). We thank all of the SeaBASS data contributors and the NASA Ocean Biology Processing Group at Goddard. We thank the SeaWiFS Project Office and NASA Goddard DAAC for providing high-resolution level 1a SeaWiFS data and SeaDAS software. Technical assistance from H. Dierssen, M. Kennelly, B. Franz, B. Beckmann and the SeaDAS support staff are gratefully acknowledged. This research was supported by a RI Space Grant/Vetlesen Climate Change Fellowship awarded to C. Mouw, a NASA Earth System Science Fellowship awarded to C. Mouw, and a NOPP PARADIGM grant awarded to L. Roststein and J. Yoder. Ideas were generated at the summer 2004 short course "Radiative Transfer and Inversion of Remotely Sensed Reflectance" course at UMaine, Darling Marine Center.